RESEARCH ARTICLE | FEBRUARY 01 2024

Temperature and bias voltage dependences of magnetic tunnel junction with FeAlSi electrode

Special Collection: Spin-Related Quantum Materials and Devices

Shoma Akamatsu **№** (0); Byung Hun Lee (0); Yasen Hou; Masakiyo Tsunoda (0); Mikihiko Oogane (0); Geoffrey S. D. Beach (0); Jagadeesh S. Moodera (0)



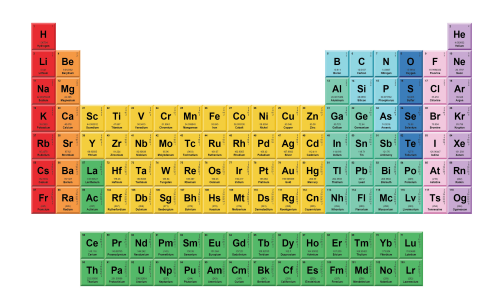
APL Mater. 12, 021101 (2024) https://doi.org/10.1063/5.0189570











American Elements
Opens a World of Possibilities
...Now Invent!
www.americanelements.com



Temperature and bias voltage dependences of magnetic tunnel junction with FeAlSi electrode

Cite as: APL Mater. 12, 021101 (2024); doi: 10.1063/5.0189570 Submitted: 29 November 2023 • Accepted: 16 January 2024 • Published Online: 1 February 2024







Shoma Akamatsu,^{1,2,a)} D Byung Hun Lee,³ D Yasen Hou,¹ Masakiyo Tsunoda,⁴ Mikihiko Oogane,^{2,5}





Geoffrey S. D. Beach, ³ and Jagadeesh S. Moodera ^{1,6}

AFFILIATIONS

- ¹ Francis Bitter Magnet Laboratory, Plasma Science and Fusion Center, Massachusetts Institute of Technology, Cambridge, Massachusetts 02139, USA
- ²Department of Applied Physics, Graduate School of Engineering, Tohoku University, Sendai 980-8579, Japan
- ³ Department of Materials Science and Engineering, Massachusetts Institute of Technology, Cambridge, Massachusetts 02139, USA
- Department of Electronic Engineering, Graduate School of Engineering, Tohoku University, Sendai 980-8579, Japan
- ⁵Center for Science and Innovation in Spintronics (Core Research Cluster) Organization for Advanced Studies, Tohoku University, Sendai 980-8577, Japan
- Department of Physics, Massachusetts Institute of Technology, Cambridge, Massachusetts 02139, USA

Note: This paper is part of the Special Topic on Spin-Related Quantum Materials and Devices.

^{a)}Author to whom correspondence should be addressed: shoma.akamatsu.p3@dc.tohoku.ac.jp

ABSTRACT

We fabricated magnetic tunnel junctions (MTJs) with FeAlSi free layers and investigated the tunnel magnetoresistance (TMR) properties. We found that the temperature and bias voltage dependences of the TMR effect in FeAlSi-MTJs were almost the same as MTJs with Fe free layers despite the low Curie temperature of FeAlSi. In the inelastic electron tunneling spectroscopy measured at low temperatures, the relatively large cutoff energy of magnon excitation at the FeAlSi and MgO interface was confirmed. In addition, we studied for the first time the exchange stiffness constant of FeAlSi films by Brillouin light scattering. The determined value of the stiffness constant of FeAlSi was 14.3 (pJ/m), which was similar to that of Fe. Both the large magnon cutoff at the interface and the stiffness constant of FeAlSi are considered to be the reason for the good temperature and voltage dependences of FeAlSi-MTJs.

© 2024 Author(s). All article content, except where otherwise noted, is licensed under a Creative Commons Attribution (CC BY) license (http://creativecommons.org/licenses/by/4.0/). https://doi.org/10.1063/5.0189570

Sendust alloy (Fe_{73.7}Al_{9.7}Si1_{6.6} atm %, henceforth "Sendust") is a famous soft magnetic material invented by Masumoto and Yamamoto in 1937. In our previous studies, ^{2,3} we demonstrated the excellent soft magnetic properties of nm-Sendust films comparable to that of bulk for the first time and discovered the mechanism of the soft magnetic properties of Sendust alloy, including bulk and film forms.² These studies suggested the possibility of applying Sendust films into a Magnetic Tunnel Junction (MTJ)-based magnetic sensor, where external magnetic fields are detected using the tunnel magnetoresistance (TMR) effect. The soft magnetic properties of ferromagnetic materials for free layers and high TMR ratios of MTJs are simultaneously required to attain a high sensitivity of MTJ-based sensor. Sendust with a good soft magnetic property can be a good

candidate for the free layer in MTJs because Sendust is expected to show a high TMR ratio. Sendust has the similar composition and crystal structure as Fe, which leads to a high TMR ratio by the effect of Δ_1 coherent tunneling. ⁴⁻⁶ We hypothesized that Δ_1 coherent tunneling would happen in MTJs using Sendust electrodes and investigated the TMR properties of MTJs using Sendust free layers. In our previous work,⁷ we successfully observed a high TMR ratio of 121% at RT, which showed the big potential of Sendust films as the free layer material for a MTJ sensor.8 To study the electronic structure of Sendust, we have also investigated the tunnel anisotropic magnetoresistance (TAMR) effect at low temperatures. The TAMR ratio is defined as the ratio between the resistance of in-plane parallel state and the resistance of out-of-plane parallel state, which provided us the information about the interfacial resonance state (IRS) of the ferromagnetic layer. We observed a TAMR ratio of $1\%^{10}$ comparable to Fe, which showed that Sendust had the IRS at the interface with MgO similar to Fe.

In this paper, we systematically studied the temperature and bias voltage (V_{Bias}) dependences of the TMR effect in MTJs with Sendust electrodes. Basically, the TMR ratio decreases with the increasing temperature and $V_{\rm Bias}$ increases, and the TMR reduction is mainly caused by magnetic fluctuations in ferromagnetic layers and the large resistance drop in the anti-parallel configuration due to the inelastic tunneling effect.⁶ The previous studies suggested that the TMR ratio reduction against temperature and bias voltage is related to magnon excitations in ferromagnetic layers. 11-15 The Curie temperature (T_c) of bulk-Sendust is previously reported as 733 K,16 which is much smaller than that of Fe (1043 K).17 As a result, this relatively low T_c can cause the large temperature and bias voltage dependences in Sendust-MTJs. Since inelastic tunneling spectroscopy (IETS) is one of the powerful tools to investigate the magnon excitation in MTJs, the IETS measurement was carried out for MTJs with Sendust electrodes in this study. In addition, although the exchange stiffness constant (A) of ferromagnetic layers also affect the temperature and bias voltage dependences in MTJs, ¹⁸ there were no studies on the A of Sendust films. In this study, we adopted the Brillouin Light Scattering (BLS) technique to directly investigate the A for Sendust. The investigations of A would also be useful for the studies of micromagnetic calculations and the spin dynamics for new spintronic materials of Sendust.

The stacking structure of the MTJ film, which was used for the temperature dependence of the TMR effect, was as follows:

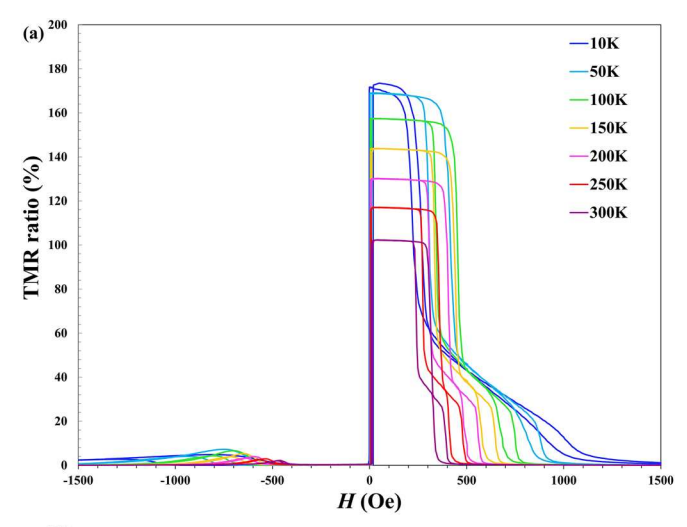
MgO(001)-substrate/MgO(20)/Sendust(30)/MgO(2)/Co₄₀Fe₄₀B₂₀ $(3)/Ru(0.85)/Co_{75}Fe_{25}(5)/Ir_{22}Mn_{78}(10)/Ta(5)/Ru(10)$ (in nm). The Fe74.8 Al11.1 Si14.1 (atm. %) films were deposited and annealed with the annealing temperature (T_a) of 400 °C. After the depositions of full stacking layers, the sample was annealed with $T_a = 325$ °C under a magnetic field of 1 T to fix the magnetization in the pinned layer, to improve the crystallinity of MgO barrier layer, ¹⁹ and to crystallize the Co-Fe-B layer. The composition of Sendust films and T_a were the optimized values in our previous study,8 where good crystallinity and (001)-orientation were confirmed using x-ray diffraction (XRD) and Transmission Electron Microscopy (TEM). In addition to the measurement for temperature dependence, the $V_{\rm Bias}$ dependence of conductance and inelastic electron tunneling spectroscopy (IETS) was also conducted using a physical property measurement system (PPMS by Quantum Design). The stacking for BLS measurements was as follows: MgO (001)-substrate/MgO(20)/Sendust(10) $T_a = 400$ °C/Ta(5). The composition of Sendust was Fe_{73.7}Al_{11.7}Si_{14.6} (atm. %), which was almost the same as that of MTJ sample. BLS was conducted following the previous work,²⁰ where a laser with a wavelength of $\lambda = 532$ nm was projected onto the surface at an angle θ from the surface normal, in a plane perpendicular to the external field H. The component of the magnon wave vector that is in-plane is oriented along the y axis, and its wave vector transfer is represented as $k = (4\pi/\lambda) \sin \theta$. The BLS results are affected by the Dzyaloshinskii–Moriya interaction (DMI), ^{22–24} which is also the first investigation for Sendust films by this study. We conducted two types of BLS measurements: H = 0.2-0.6 T with $\theta = 0^{\circ}$ and $\theta = 0^{\circ} - 45^{\circ}$ with H = 0.2 T. We can determine A based on those two measurements and the following equation:

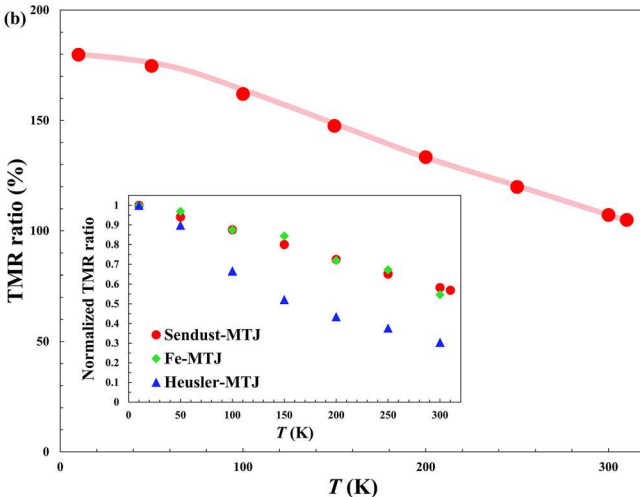
$$f_{DE} = \frac{\mu_0 \gamma}{2\pi} \sqrt{H[H + H_{k_{eff}}] + \left(\frac{M_s}{2}\right)^2 (1 - \exp(-2kt))} \pm \frac{2\gamma}{2\pi M_s} Dk,$$
 (1)

$$f_{PSSW} = \frac{\mu_0 \gamma}{2\pi} \sqrt{\left[H + \frac{2A}{\mu_0 M_s} \left(k^2 + \left(\frac{n\pi}{t}\right)^2\right)\right] \left[H + \frac{2A}{\mu_0 M_s} \left(k^2 + \left(\frac{n\pi}{t}\right)^2\right) + H_{k_{eff}}\right]},$$
 (2)

where $f_{\rm DE}$ and $f_{\rm PSSW}$ are the frequencies of Damon–Eshbach (DE) mode and Perpendicular Standing Spin Wave (PSSW) mode, respectively, γ is the gyromagnetic ratio, H is the external field (in-plane), $M_{\rm s}$ is the saturation magnetization, $H_{\rm k_eff}$ is the effective in-plane anisotropy field, and D is a DMI constant. The fitting parameters were $\gamma/2\pi$ (GHz/T), $\mu_0H_{\rm k_eff}$ (T), A (pJ/m), and t, where t was included to determine the thickness of Sendust exactly. The sample for BLS was also measured using a vibrating sample magnetometer (VSM) to determine $M_{\rm s}$ for the prepared sample.

Figure 1(a) shows the temperature dependence of magnetoresistance curves for an MTJ using the Sendust free layer. Figure 1(b) summarizes the temperature dependence of TMR ratio, and the inset shows the normalized TMR ratio (TMR ratio/TMR ratio @10 K). We confirmed that the TMR ratio increased monotonously from 104.8% at 300 K to 179.8% at 10 K, and the ratio of (TMR ratio at 300 K) to (TMR ratio at 10 K) is 0.58. In other previous studies of MTJs using Fe electrodes,²⁷ the TMR ratio also increased monotonously, from 170% at 300 K to 318% at 10 K. The (TMR ratio at 300 K)/(TMR ratio at 10 K) ratio for Fe-MTJs is 0.53, which is similar to Sendust-MTJs in our study. These results show that the temperature dependence of TMR ratio for Sendust-MTJs and Fe-MTJs is almost the same. Meanwhile, the (TMR ratio at 300 K)/(TMR ratio at 10 K) ratio for Heusler-MTJs in other previous studies is much lower than these values (0.31).²⁸ This large temperature dependence of TMR ratio is affected by the reduction in spin polarization at the interface of Heusler alloys. 28 These results proved the thermal stability of TMR ratio and spin polarization in Sendust-MTJs comparable to Fe-MTJs. Figure 1(c) shows the temperature dependence of resistance-area (RA) product for the parallel (RA_P) and anti-parallel (RA_{AP}) configurations. We found that the temperature dependence of RA_{AP} is much larger than that of RA_P similar to previous studies. 6,27,29,30 The increase in RA_{AP} with a decrease in





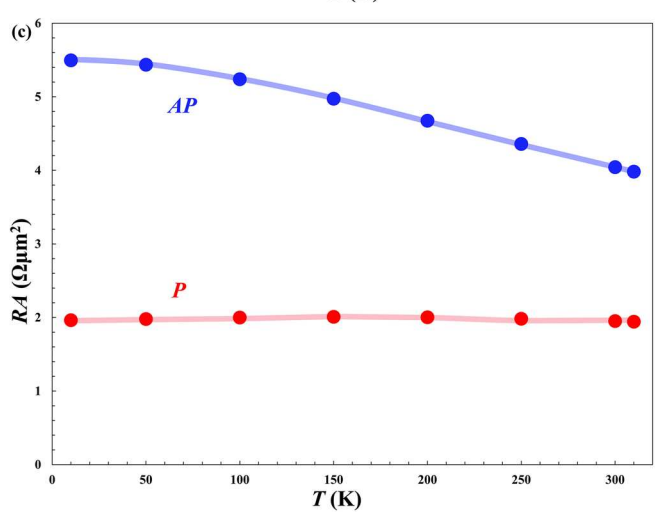


FIG. 1. Temperature dependence of (a) magnetoresistance curve; inset: TMR ratio normalized by the value @10 K compared with other MTJs, (b) TMR ratio, and (c) $R_{\rm P}$ and $R_{\rm AP}$ for MTJs using Sendust electrodes.

temperature is considered to be the suppression of spin-flip tunneling caused by magnon excitations at the interface between Sendust and MgO. 31

Figure 2(a) shows the V_{Bias} dependence of TMR ratio evaluated by dI/dV-V curves for the parallel and anti-parallel magnetic configurations in Sendust-MTJs shown in Fig. 1. The TMR ratio drop with a finite $V_{\rm Bias}$ is considered to be mainly affected by the magnon excitation. V_{half}, which is the $V_{\rm Bias}$ where the TMR ratio is half of that at $V_{\rm Bias} = 0$ V, is about 300 mV. This value is almost the same as a previous study for Fe-MTJs.³² Both the temperature and bias-voltage dependences of the TMR effect for the Sendust- and Fe-MTJs are almost the same, which indicates that the Sendust/MgO interface appears to behave similar to the Fe/MgO interface. For investigating the magnon excitation at the Sendust/MgO interface in detail, we measured the IETS for the AP state at 1.6 K using PPMS [Fig. 2(b)]. We successfully measured the IETS with very low noise, which allowed us to observe various clear peaks. The peak around $V_{\rm Bias} \sim 80~{\rm mV}$ is supposed to be caused by the phonon excitation in the MgO barrier, which is typically observed in some previous studies.^{33–35} The strong peak at $V_{\rm Bias} \sim 30~{\rm mV}$ is considered to be originating from the magnon excitation.³⁴ This is supposed to be related to the temperature dependence of RAAP in Fig. 1(c). In Fig. 2(b), this magnon contribution exists up to $V_{\rm Bias} = 150-200$ mV, which is comparable to Fe-MTJs (150–200 mV)^{9,36} and larger than Heusler-MTJs (<100 mV).³⁴ This voltage is called maximum magnon cutoff energy $E_{\rm m}$, 37 which is related to T_c as follows:

$$E_m = \frac{3k_B T_c}{S+1},\tag{3}$$

where S is the spin of a ferromagnet. T_c for Sendust is calculated to be about 1000 K from Eq. (3), which is similar to Fe (1043 K¹⁷). The evaluated large T_c of Sendust comparable to Fe corresponds to the small temperature dependence of TMR ratio and high $V_{\rm half}$. However, the estimated T_c of 1000 K in Sendust-MTJs is obviously higher than a previous report of T_c for Sendust (733 K¹⁶). The first possible reason for high T_c of Sendust is that the composition and the atomic ordering of Sendust films in this work are different from a previous study. The second possible reason is that the composition of Sendust at the interface with MgO barrier is Fe-rich because of diffusion of Si and Al atoms during the annealing process.

Next, we investigated the A by BLS and its relationship with the temperature dependence of TMR ratio. Figure 3 shows the magnetization curve of the Sendust sample prepared for BLS measurements. The measured coercivity is less than 1 Oe similar to our previous studies, ^{2.8} which means that we successfully fabricated Sendust films with ideal soft magnetic properties. M_s is identified to be 0.0011 emu, so we can determine the $M_s t$ value of 0.0012 emu/cm² (the sputtered area was 0.92 cm²), which are used for fitting with Eqs. (1) and (2).

Figure 4 shows the results of BLS measurements for the prepared Sendust film, where we clearly observed the DE and PSSW mode peaks. We only find the PSSW mode (n = 1) because PSSW modes (n \geq 2) are too weak as their thickness is thin (10 nm). Both peaks of DE and PSSW modes increase with a higher H in Fig. 4(a), whereas almost only the DE mode peak increases with a higher θ (k) in Fig. 4(b), as theoretically predicted and shown in Eqs. (1) and (2). Figure 4(c) shows the k dependence of the difference between the

APL Materials

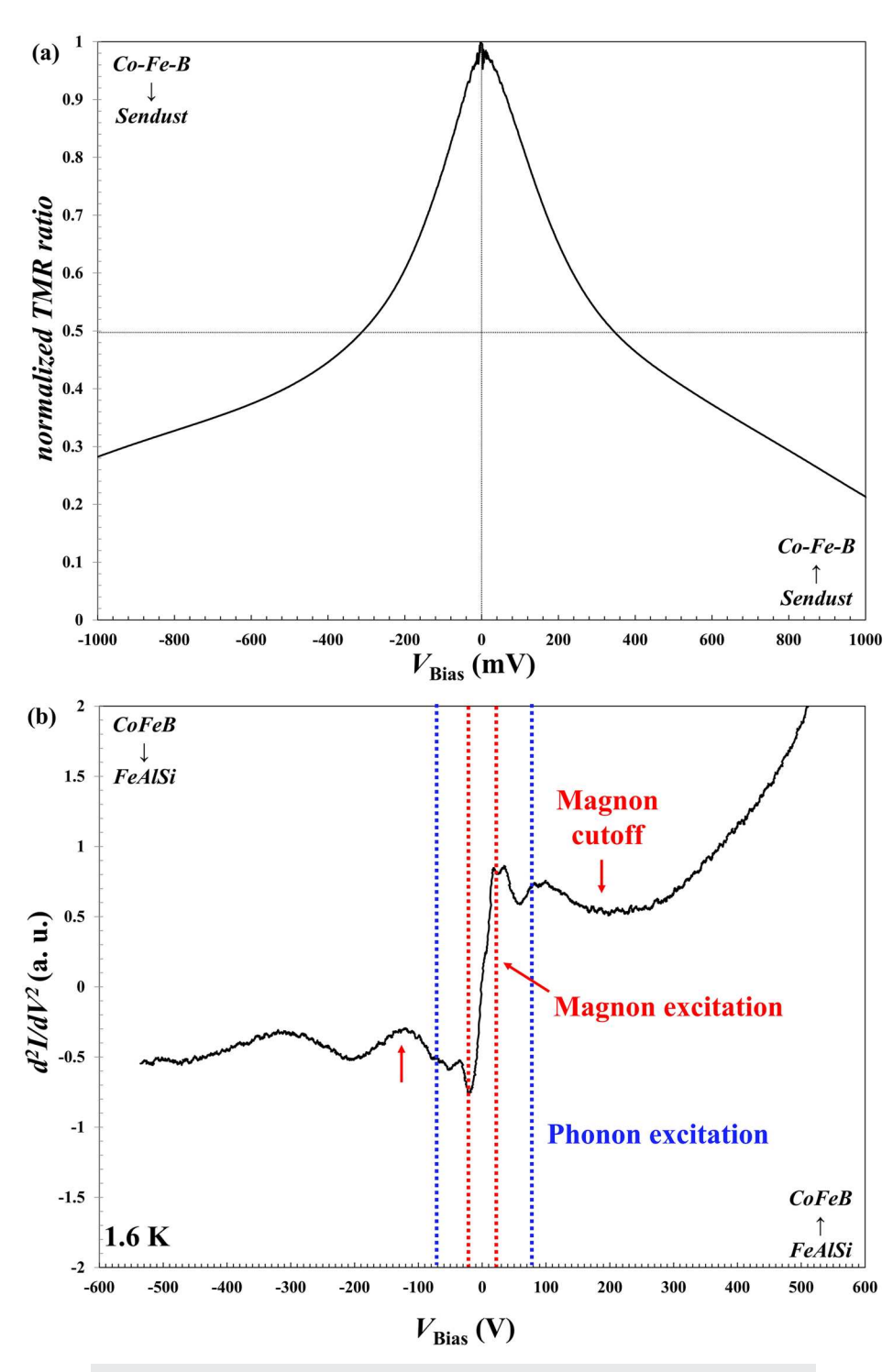


FIG. 2. V_{Bias} dependence of the (a) TMR ratio and (b) IETS for AP configuration measured at 1.6 K.

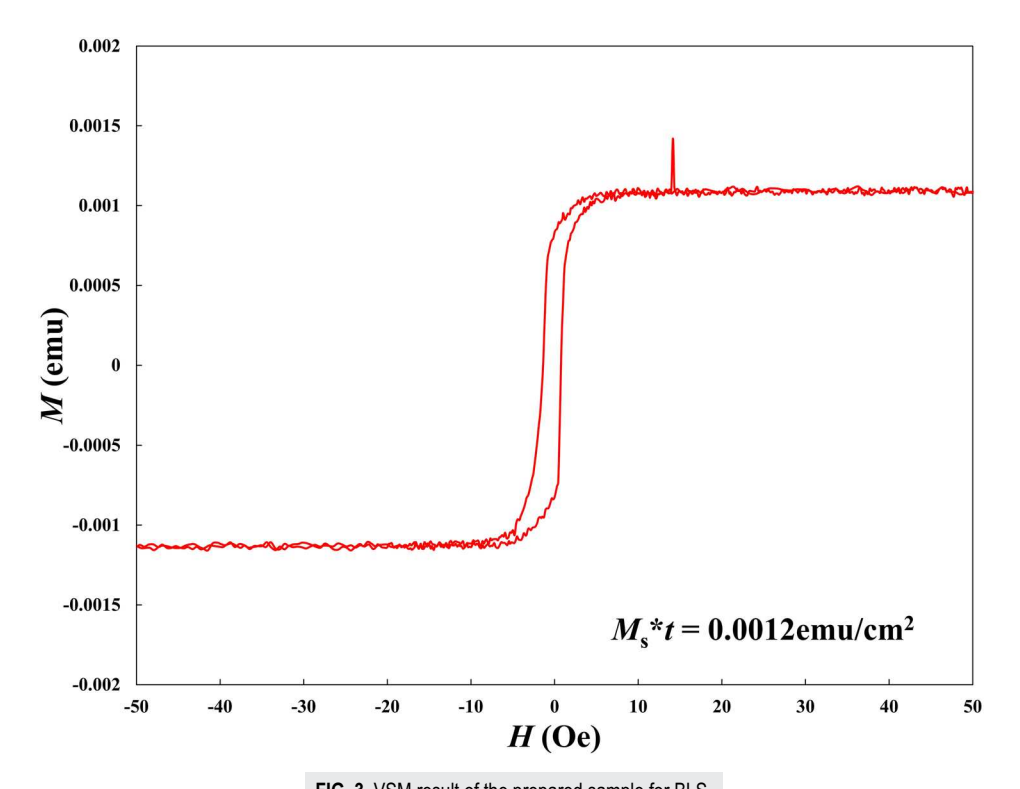


FIG. 3. VSM result of the prepared sample for BLS.

Stokes (S) peak (negative frequency) and the anti-Stokes (AS) peak (positive frequency) defined as follows:³⁸

$$\Delta f_{DE} = f_S - f_{AS} = \frac{2\gamma}{\pi M_s} Dk. \tag{4}$$

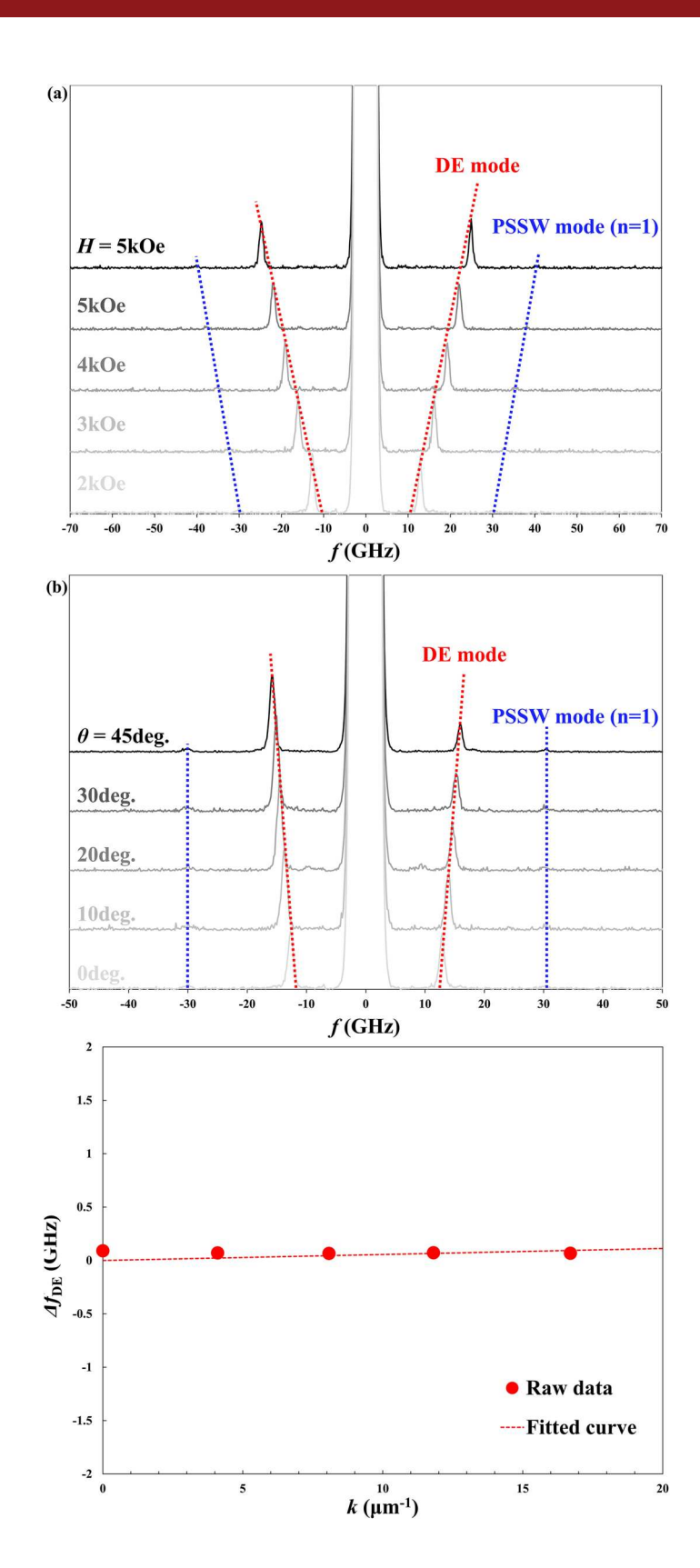
We tried the fitting of raw data using Eq. (4). The calculated D was $4.5 \pm 1.9 \, (\mu J/m^2)$, which suggests negligible DMI values because of small value with a relatively large error. This result corresponds to that we could not observe a linear behavior in Fig. 4(c). Therefore, we conclude that there is no DMI in Sendust films.

Since there is no difference between the Stokes peak and the anti-Stokes peak, we summarized only the Stokes peak's dependence on H and k in Figs. 5(a) and 5(b), respectively. We fitted both DE and PSSW mode peaks using Eqs. (1) and (2), respectively and determined the film thickness and various magnetic constants (Table I). We confirm the reasonable thickness of 9.95 nm comparable to that determined during film growth, which means that our fittings are successful. The estimated A for Sendust was 14.3 (pJ/m), which is the first time determination of A of Sendust film.

Finally, we summarize A, T_c , (TMR@300 K)/(TMR@10 K), and $E_{\rm m}$ for Sendust and Fe in Table II, where all these values should be correlated as mentioned in this paper. The results for Sendust and Fe are similar except for T_c , and this reason for discrepancy of T_c is already mentioned previously. Further investigation is needed to

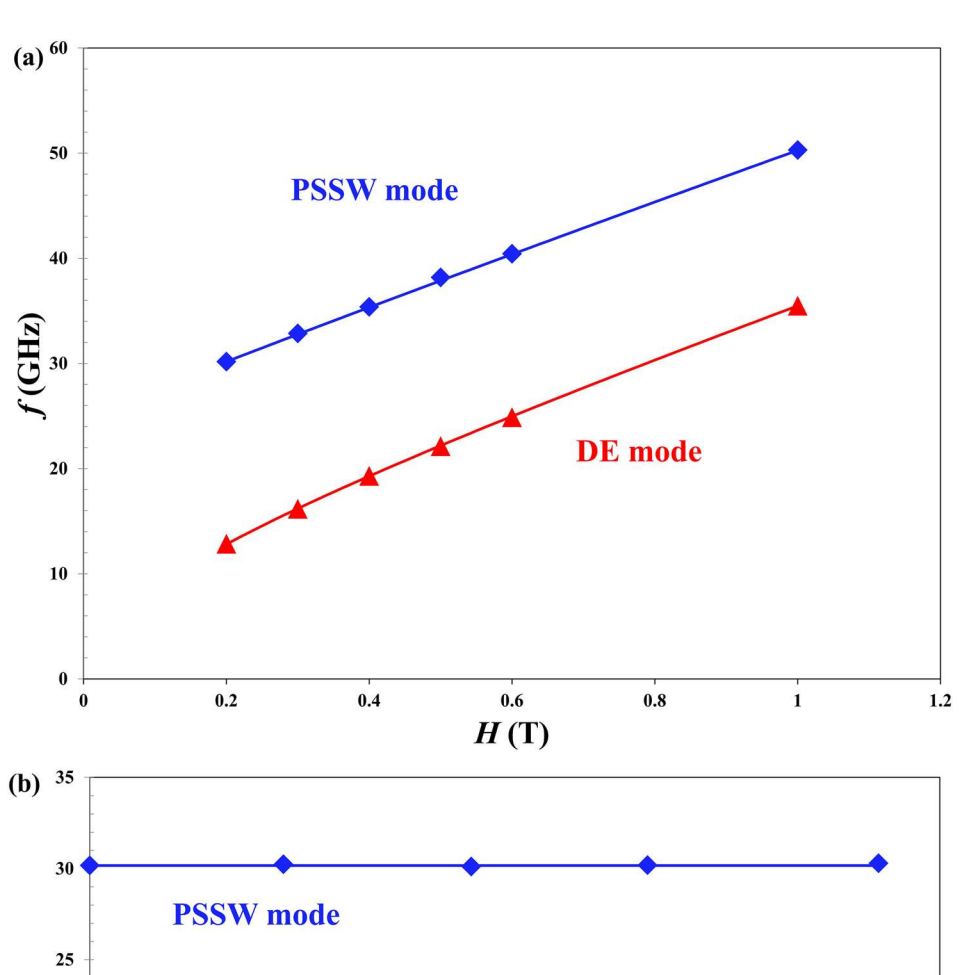
clarify this point. Our study also revealed that TMR reduction with finite T and $V_{\rm Bias}$ in Sendust-MTJs is significantly lower than that in Heusler-MTJs. The reason of the large TMR reduction in Heusler-MTJs despite a large A ($T_{\rm c}$) is considered to be due to the local A ($T_{\rm c}$) reduction at the interface with MgO, $^{31-33}$ and thus, we understand that there is minimal such effect in Sendust-MTJs.

In summary, we carried out the investigation on the temperature and bias-voltage dependences of the TMR effect in MTJs with Sendust electrodes. The temperature dependence of TMR ratio for MTJs using Sendust free layers behaved similar to the MTJs using Fe electrodes, where the (TMR ratio at 300 K)/(TMR ratio at 10 K) ratio for Sendust- and Fe-MTJs was 0.58 and 0.53, respectively. The V_{Bias} dependence of TMR ratio for Sendust-MTJs was also similar to that of Fe-MTJs, where both V_{half} values were about 300 mV. By measuring the IETS for Sendust-MTJs, we observed the peak that was considered to have originated from the magnon excitation of Sendust interface with MgO, and the observed $E_{\rm m}$ was comparable to that of MTJs with an Fe electrode. BLS measurements provided us the first information about A in Sendust films. The identified value was 14.3 (pJ/m), which was almost the same as the previous studies of Fe. These large Em and stiffness constant are consistent with the observed small temperature and bias-voltage dependences of the TMR effect in Sendust-MTJs. The lower temperature and bias-voltage dependences in MTJs with Sendust electrodes are highly beneficial for their application as TMR sensors with a large sensitivity.



 $\textbf{FIG. 4.} \ \, \text{BLS results for (a)} \ \, \textit{H} \ \, \text{dependence and (b)} \ \, \textit{k} \\ \, \text{dependence. (c) Evaluation for DMI in Sendust films.}$

APL Materials



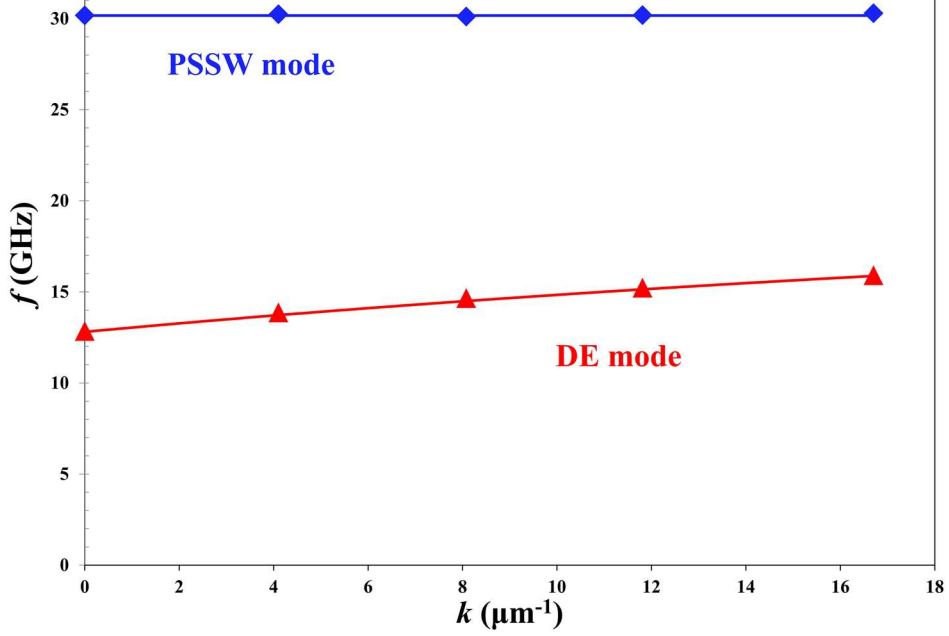


FIG. 5. Peak position and fitting results for BLS.

TABLE I. Fitting results for γ , H_{k} eff, and A for the prepared Sendust films.

t (nm)	$\frac{\gamma}{2\pi}(GHz/T)$	$\mu_0 H_{k_eff}$ (T)	A (pJ/m)
9.95	23.4	1.3	14.3

TABLE II. Summary of *A* and temperature dependence of TMR ratio for Sendust, Fe, and Heusler alloy.

Ferromagnetic material	<i>T</i> _c (K)	A (pJ/m)	(TMR@300 K)/ (TMR@10 K)	E _m (meV)
Sendust	733 ¹⁶	14.3	0.58	150-200
Fe	1043^{17}	18.5^{39}	0.53^{27}	$150-200^{9,36}$
Heusler alloy	985^{18}	23.5^{18}	0.31^{28}	<100 ³⁴

This work at MIT was supported by the Air Force Office of Sponsored Research (Grant No. FA9550-23-1-0004 DEF), Office of Naval Research (Grant No. N00014-20-1-2306), National Science Foundation (Grant Nos. NSF-DMR 1700137 and 2218550), and Army Research Office (Grant Nos. W911NF-20-2-0061 and DURIP W911NF-20-1-0074). S.A.'s visit to MIT was facilitated by the Japan Society for the Promotion of Science (JSPS), Grants-in-Aid for Scientific Research, SIP project, NEDO leading project, X-NICS project, and the GP-Spin, CIES, and Center for Science and Innovation in Spintronics (CSIS) in Tohoku University.

AUTHOR DECLARATIONS

Conflict of Interest

The authors have no conflicts to disclose.

Author Contributions

Shoma Akamatsu: Conceptualization (equal); Data curation (equal); Formal analysis (equal); Funding acquisition (equal); Investigation (lead); Methodology (lead); Project administration (lead); Resources (lead); Software (lead); Validation (lead); Visualization (lead); Writing – original draft (lead). Byung Hun Lee: Data curation (equal); Formal analysis (equal). Yasen Hou: Data curation (equal). Masakiyo Tsunoda: Writing – review & editing (equal). Mikihiko Oogane: Conceptualization (equal); Funding acquisition (equal); Supervision (equal); Writing – review & editing (equal). Geoffrey S. D. Beach: Funding acquisition (equal); Supervision (equal); Writing – review & editing (equal). Jagadeesh S Moodera: Conceptualization (equal); Funding acquisition (equal); Supervision (equal); Writing – review & editing (equal).

DATA AVAILABILITY

The data that support the findings of this study are available from the corresponding author upon reasonable request.

REFERENCES

- ¹ H. Masumoto and T. Yamamoto, "On a new alloy 'Sendust' and its magnetic and electric properties," J. Japan Inst. Metals 1, 127–135 (1937).
- ²S. Akamatsu, M. Oogane, M. Tsunoda, and Y. Ando, "Guidelines for attaining optimal soft magnetic properties in FeAlSi films," Appl. Phys. Lett. 120(24), 242406 (2022).
- ³S. Akamatsu, M. Oogane, M. Tsunoda, and Y. Ando, "Fabrication of soft-magnetic FeAlSi thin films with nm-order thickness for the free layer of magnetic tunnel junction based sensors," AIP Adv. 10, 015302 (2020).
- ⁴W. H. Butler, X.-G. Zhang, T. C. Schulthess, and J. M. MacLaren, "Spin-dependent tunneling conductance of Fe|MgO|Fe sandwiches," Phys. Rev. B **63**(5), 054416 (2001).
- ⁵S. Yuasa, T. Nagahama, A. Fukushima, Y. Suzuki, and K. Ando, "Giant room-temperature magnetoresistance in single-crystal Fe/MgO/Fe magnetic tunnel junctions," Nat. Mater. 3(12), 868–871 (2004).
- ⁶S. S. P. Parkin, C. Kaiser, A. Panchula, P. M. Rice, B. Hughes, M. Samant, and S.-H. Yang, "Giant tunnelling magnetoresistance at room temperature with MgO (100) tunnel barriers," Nat. Mater. 3(12), 862–867 (2004).
- ⁷S. Akamatsu, M. Oogane, Z. Jin, M. Tsunoda, and Y. Ando, "Tunnel magnetoresistance in magnetic tunnel junctions with FeAlSi electrode," AIP Adv. 11(4), 045027 (2021).
- ⁸S. Akamatsu, M. Oogane, M. Tsunoda, and Y. Ando, "Magnetic tunnel junctions using epitaxially grown FeAlSi electrode with soft magnetic property," AIP Adv. **12**(7), 075021 (2022).
- ⁹Y. Lu, H.-X. Yang, C. Tiusan, M. Hehn, M. Chshiev, A. Duluard, B. Kierren, G. Lengaigne, D. Lacour, C. Bellouard, and F. Montaigne, "Spin-orbit coupling effect by minority interface resonance states in single-crystal magnetic tunnel junctions," Phys. Rev. B 86(18), 184420 (2012).
- ¹⁰S. Akamatsu, T. Nakano, M. Al-Mahdawi, W. Yupeng, M. Tsunoda, Y. Ando, and M. Oogane, "Tunnel anisotropic magnetoresistance in magnetic tunnel junctions using FeAlSi," AIP Adv. 13(2), 025005 (2023).
- ¹¹ M. Ležaić, P. Mavropoulos, and S. Blügel, "First-principles prediction of high Curie temperature for ferromagnetic bcc-Co and bcc-FeCo alloys and its relevance to tunneling magnetoresistance," Appl. Phys. Lett. **90**, 082504 (2007).
- ¹²C. H. Shang, J. Nowak, R. Jansen, and J. S. Moodera, "Temperature dependence of magnetoresistance and surface magnetization in ferromagnetic tunnel junctions," Phys. Rev. B 58(6), R2917–R2920 (1998).
- ¹³R. J. M. van de Veerdonk, J. S. Moodera, and W. J. M. de Jonge, "Characterization of magnetic tunnel junctions using IETS," J. Magn. Magn. Mater. 198–199, 152–154 (1999).
- ¹⁴J. S. Moodera, J. Nowak, and R. J. M. van de Veerdonk, "Interface magnetism and spin wave scattering in ferromagnet-insulator-ferromagnet tunnel junctions," Phys. Rev. Lett. 80(13), 2941–2944 (1998).
- ¹⁵J. S. Moodera, L. R. Kinder, T. M. Wong, and R. Meservey, "Large magnetore-sistance at room temperature in ferromagnetic thin film tunnel junctions," Phys. Rev. Lett. 74(16), 3273–3276 (1995).
- ¹⁶W. Wang, T. Ma, and M. Yan, "Microstructure and magnetic properties of nanocrystalline Co-doped Sendust alloys prepared by melt spinning," J. Alloys Compd. **459**(1–2), 447–451 (2008).
- ¹⁷C. Kittel and P. McEuen, *Introduction to Solid State Physics* (Wiley, 2018).
- 18 T. Kubota, J. Hamrle, Y. Sakuraba, and O. Gaier, "Structure, exchange stiffness, and magnetic anisotropy of $Co_2MnAl_xSi_{1-x}$ Heusler compounds," J. Appl. Phys. **106**, 113907 (2009).
- ¹⁹W. H. Meiklejohn and C. P. Bean, "New magnetic anisotropy," Phys. Rev. 102, 1413 (1956).
- ²⁰B. H. Lee, T. Fakhrul, C. A. Ross, and G. S. D. Beach, "Large anomalous frequency shift in perpendicular standing spin wave modes in BiYIG films induced by thin metallic overlayers," Phys. Rev. Lett. 130(12), 126703 (2023).
- ²¹T. Sebastian, K. Schultheiss, B. Obry, B. Hillebrands, and H. Schultheiss, "Micro-focused Brillouin light scattering: Imaging spin waves at the nanoscale," Front. Phys. **3**, 35 (2015).
- ²²S. Ding, A. Ross, R. Lebrun, S. Becker, K. Lee, I. Boventer, S. Das, Y. Kurokawa, S. Gupta, J. Yang, G. Jakob, and M. Kläui, "Interfacial Dzyaloshinskii-Moriya interaction and chiral magnetic textures in a ferrimagnetic insulator," Phys. Rev. B 100(10), 100406 (2019).

- ²³ A. J. Lee, A. S. Ahmed, J. Flores, S. Guo, B. Wang, N. Bagués, D. W. McComb, and F. Yang, "Probing the source of the interfacial Dzyaloshinskii-Moriya interaction responsible for the topological Hall effect in Metal/Tm₃Fe₅O₁₂ systems," Phys. Rev. Lett. 124(10), 107201 (2020).
- ²⁴L. Caretta, E. Rosenberg, F. Büttner, T. Fakhrul, P. Gargiani, M. Valvidares, Z. Chen, P. Reddy, D. A. Muller, C. A. Ross, and G. S. D. Beach, "Interfacial Dzyaloshinskii-Moriya interaction arising from rare-earth orbital magnetism in insulating magnetic oxides," Nat. Commun. 11(1), 1090 (2020).
- ²⁵B. A. Kalinikos and A. N. Slavin, "Theory of dipole-exchange spin wave spectrum for ferromagnetic films with mixed exchange boundary conditions," J. Phys. C: Solid State Phys. 19(35), 7013 (1986).
- ²⁶S. O. Demokritov, B. Hillebrands, and A. N. Slavin, "Brillouin light scattering studies of confined spin waves: Linear and nonlinear confinement," Phys. Rep. **348**(6), 441–489 (2001).
- ²⁷S. G. Wang, R. C. C. Ward, G. X. Du, X. F. Han, C. Wang, and A. Kohn, "Temperature dependence of giant tunnel magnetoresistance in epitaxial Fe/MgO/Fe magnetic tunnel junctions," Phys. Rev. B 78(18), 180411 (2008).
- ²⁸S. Tsunegi, Y. Sakuraba, M. Oogane, K. Takanashi, and Y. Ando, "Large tunnel magnetoresistance in magnetic tunnel junctions using a Co₂MnSi Heusler alloy electrode and a MgO barrier," Appl. Phys. Lett. **93**(11), 112506 (2008).
- ²⁹J. Hayakawa, S. Ikeda, Y. M. Lee, F. Matsukura, and H. Ohno, "Effect of high annealing temperature on giant tunnel magnetoresistance ratio of CoFeB/MgO/CoFeB magnetic tunnel junctions," Appl. Phys. Lett. **89**, 232510 (2006); arXiv:cond-mat/0610526.
- ³⁰S. Yuasa, A. Fukushima, H. Kubota, Y. Suzuki, and K. Ando, "Giant tunneling magnetoresistance up to 410% at room temperature in fully epitaxial Co/MgO/Co magnetic tunnel junctions with bcc Co(001) electrodes," Appl. Phys. Lett. **89**(4), 042505 (2006).

- ³¹S. Zhang, P. M. Levy, A. C. Marley, and S. S. P. Parkin, "Quenching of magnetoresistance by hot electrons in magnetic tunnel junctions," Phys. Rev. Lett. **79**(19), 3744–3747 (1997).
- ³²G. X. Miao, Y. J. Park, J. S. Moodera, M. Seibt, G. Eilers, and M. Münzenberg, "Disturbance of tunneling coherence by oxygen vacancy in epitaxial Fe/MgO/Fe magnetic tunnel junctions," Phys. Rev. Lett. **100**(24), 246803 (2008).
- ³³G. X. Miao, K. B. Chetry, A. Gupta, and W. H. Butler, "Inelastic tunneling spectroscopy of magnetic tunnel junctions based on CoFeB/MgO/CoFeB with Mg insertion layer," J. Appl. Phys. 99, 08T305 (2006).
- ³⁴V. Drewello, D. Ebke, M. Schäfers, Z. Kugler, G. Reiss, and A. Thomas, "Magnon excitation and temperature dependent transport properties in magnetic tunnel junctions with Heusler compound electrodes," J. Appl. Phys. **111**(7), 07C701 (2012).
- ³⁵P. A. Thiry, M. Liehr, J. J. Pireaux, and R. Caudano, "Infrared optical constants of insulators determined by high-resolution electron-energy-loss spectroscopy," Phys. Rev. B **29**(8), 4824–4826 (1984).
- ³⁶S. G. Wang, R. C. C. Ward, T. Hesjedal, X. G. Zhang, C. Wang, A. Kohn, Q. L. Ma, J. Zhang, H. F. Liu, and X. F. Han, "Interface characterization of epitaxial Fe/MgO/Fe magnetic tunnel junctions," J. Nanosci. Nanotechnol. 12(2), 1006–1023 (2012).
- ³⁷Y. Ando, J. Murai, H. Kubota, and T. Miyazaki, "Magnon-assisted inelastic excitation spectra of a ferromagnetic tunnel junction," J. Appl. Phys. 87(9), 5209–5211 (2000).
- ³⁸K. Di, V. L. Zhang, H. S. Lim, S. C. Ng, M. H. Kuok, X. Qiu, and H. Yang, "Asymmetric spin-wave dispersion due to Dzyaloshinskii-Moriya interaction in an ultrathin Pt/CoFeB film," Appl. Phys. Lett. **106**, 052403 (2014); arXiv:1412.3907.
- ³⁹C. Vittoria, J. J. Krebs, and G. A. Prinz, "Spinwave resonance in MBE grown iron films," J. Magn. Magn. Mater. 37(2), L111–L115 (1983).